

Multifunctional hybrid nanosystem for molecular imaging applications

Sanction Order No. & Date: BT/ PR10874/ NNT/ 28/ 136/ 2008 Dated. 06.02.2009

Comprehensive progress report (2009 – 2012)

**Principal Investigator : Dr.P.Deb,
Associate Professor
Department of Physics
Tezpur University (Central University)
Tezpur-784028**

DEPARTMENT OF BIOTECHNOLOGY

MINISTRY OF SCIENCE AND TECHNOLOGY

Block-2, CGO Complex, Lodhi Road, New Delhi 110003.

Scientific and Technical Progress Report (STPR)

(R & D Projects)

Section A: Project Details

A1. Project Title: **Multifunctional Hybrid Nanosystem For Molecular Imaging Applications**

A2. DBT Sanction Order No. & Date:

BT/PR10874/NNT/28/136/2008 Dated. 06.02.2009

A3. Principal Investigator : Dr. P. Deb, Department of Physics, T.U.

Co-Investigators : Dr. E. Kalita, Department of MBBT, T.U.
: Dr. Gautam Kr. Goswami, Gauhati Medical College
: Dr. Dipu Bhuyan, Gauhati Medical College.

A4. Institute : **TEZPUR UNIVERSITY (CENTRAL UNIVERSITY),
TEZPUR**

A5. Address with contact nos.

(Landline & Mobile) & E-mail:

Dr. P. Deb
Principal Investigator
& Associate Professor
Department of Physics
Tezpur University (Central University)
Napaam, Tezpur 784028
Ph. 03712 27 5560
Fax . 03712-267005, 267006
Email : pdeb@tezu.ernet.in

A6. Total cost : Rs.363.09 lakh

A7. Duration : 2009-12 (3 years)

A8. Approved objectives of the project:

6 months	➤ Literature survey and procurement of instruments.
12 months	➤ Characterization of microstructural and physical properties of SPIONs to be used for conjugation in the hybrid nanosystem. ➤ Characterization of the emission spectrum of the QDs synthesized on size dependent basis.
18 months	➤ Stable conjugation of the single / multimeric QDs with SPIONs to develop a functional nanosystem
24 months	➤ Identification of the biocompatible agent most suited for coating the hybrid nanosystem. ➤ Characterization of the magnetic, optical and microstructural properties of the hybrid nanosystem ➤ Construction of SPION-QD precursor library
30 months	➤ Evaluating the extent of enhanced uptake of the hybrid nanosystem after surface modification ➤ Investigation of the level of cytotoxicity, biostability and inflammatory response of the biocompatible hybrid nanosystem in cellular/biological systems
36 months	➤ Assessment of the novel contrast agents in terms of florescence and magnetic imaging capabilities in cellular/biological systems.

A9. Specific Recommendations made by the

Task Force (if any).

: Satisfactory and recommended for acceptance of the report (07-09-2012)

DBT has granted sanctions for our project proposal entitled "Multifunctional hybrid nanosystems for molecular imaging applications" vide letter no. BT/PR10874/NNT/28/136/2008 dated 06.02.2009 through the sanction (No. Grant/DBT/CSH/GIA/2598/2008-2009 dated 13.03.2009) for the implementation of the project.

Contents

Page No.

1	Achieved objectives	5
2	Results and Discussion	5
2.1	Synthesis and characterization of iron rich Fe_xPt_{1-x} ferrofluid for magnetic resonance imaging.	5
2.2	Simple synthesis of highly efficient contrast agent of magnetite nanoparticles with controllable surface functionality	8
2.3	High luminescence biocompatible multimodal ZnSe(S) nanodots for biomedical applications.	10
2.4	Differential tunability effect on the optical properties of doped and undoped quantum dots.	12
2.5	Direct monophasic replacement of fatty acid by DMSA on SPION surface.	14
2.6	Simple synthesis of superparamagnetic magnetite nanoparticles as highly efficient contrast agent	16
2.7	Enhanced Quantum Confined Stark Effect in a Mesoporous hybrid multifunctional system	18
2.8	Sensitive fluorescence response of ZnSe(S) quantum dots: an efficient fluorescence probe	20
2.9	Significant improvement in dopant emission and lifetime in water soluble Cu:ZnSe/ZnS nanocrystals	21
2.10	Single moiety, multifunctional iron-platinum nanoparticles for potential MR imaging and therapeutic applications	23
2.11	Hierarchically architected multifunctional mesoporous maglumino hybrids	25
3	Summary & Conclusion	27
4	Details of new leads obtained	27
5	Outcomes of the project	28
6	Instruments procured and installed	33

1. Achieved objectives

- (i) Development of library of magnetic nanoparticles, quantum dots (fluorescent probes) and magneto-fluorescent hybrid nanosystems for molecular imaging applications.
- (ii) Thirteen papers
- (iii) Two patents applied
- (iv) Two software copyrights granted

Development of Process/product/technology attempted in this project-

- Development of hybrid nanosystems having multifunctional characteristics- fluorescent imaging, MR imaging, drug delivery and targeted protein binding, is an unique outcome of the project

2. Results and Discussion

2.1. Synthesis and characterization of iron rich $\text{Fe}_x\text{Pt}_{1-x}$ ferrofluid for magnetic resonance imaging

Abstract

Iron rich $\text{Fe}_x\text{Pt}_{1-x}$ ultrafine nanodots were prepared by a simple and versatile polyol process using a combinatorial strategy of introducing a strong reducing agent and decreasing synthesis temperature. The native hydrophobic nanodots were converted to a wettable dispersion by ligand exchange mediated phase transformation using tetramethyl ammonium hydroxide (TMAOH). The microstructural study confirmed the formation of the Fe-rich FePt nanodots having an average particle size of ~ 3.5 nm with a narrow size distribution. The MTT study on mammalian leukocyte cultures confirmed high degree of biocompatibility for the ferrofluid. The ferrofluid when studied for its concentration dependent transverse relaxation time and contrast properties was found to exhibit promising properties as MRI T_2 contrast agent.

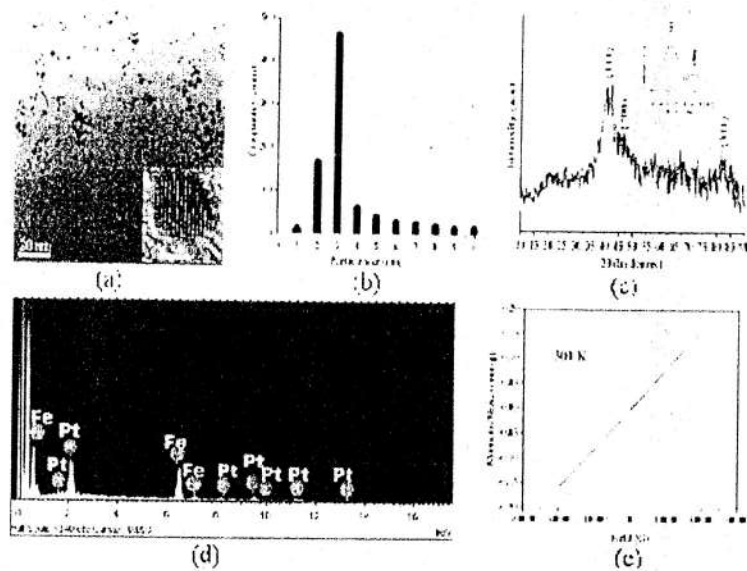


Figure 1 (a) HR-TEM micrograph (inset showing nanodot), (b) Estimated size distribution, (c) XRD pattern (inset showing deconvoluted main peak), (d) EDX pattern and (e) Room temperature hysteresis behavior of hydrophilic FePt nanodots.

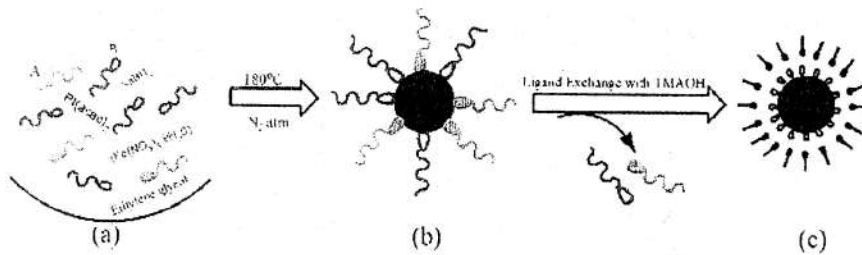


Figure 2 The schematic diagram represents the synthesis and ligand exchange of FePt nanodots. (a) Precursors [Oleic acid (A) and Oleylamine (B)], (b) Oleic acid and Oleylamine@FePt and (c) TMAOH @ FePt . The surface capping is composed of (OH⁻) anions (⊖) and (CH₃)₄N⁺) cation (⊕).

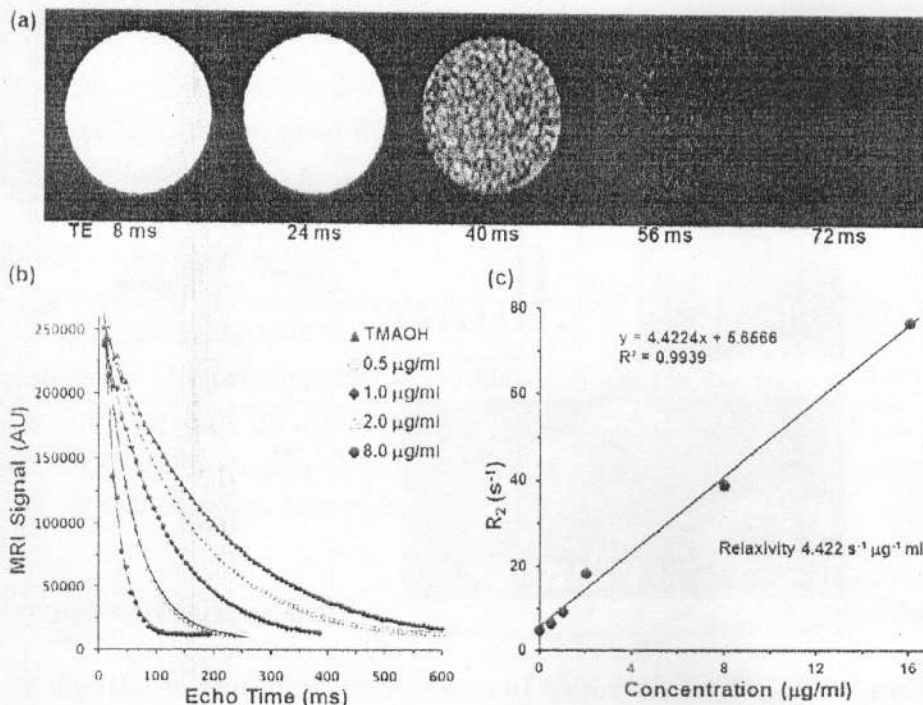


Figure 3 Measurement of transverse relaxivity of FePt nanodots. (a) MRI image of microfluidic tube containing FePt nanodots in water at different echo time (8, 24, 40, 56 and 72 ms), (b) Plot of MR image intensity vs echo time for estimation of transverse relaxation time (T_2) and (c) Variation in transverse relaxation rate w. r. t. nanodot concentrations.

Conclusion: we have developed a biocompatible ferrofluid for magnetic imaging, comprising of iron-rich FePt nanodots. The native $\text{Fe}_x\text{Pt}_{1-x}$ ($x=0.7$) nanodots were surface modified to bring about the hydrophobic-hydrophilic phase transformation. Our results provide an alternative approach to synthesize high quality nanoparticles using the polyol process and yet achieve wettable dispersions with high biocompatibility characteristics. Further, the contrast enhancement of the ferrofluid makes it a potential T_2 contrast agent for MRI application.

2.2 Simple synthesis of highly efficient contrast agent of magnetite nanoparticles with controllable surface functionality

Abstract

Magnetite (Fe_3O_4) nanoparticles have been prepared by one-pot thermal decomposition process using iron (III) acetylacetonate in stearic acid in ambient environment. In this process stearic acid acts as both solvent as well as capping agent. These as-prepared hydrophobic magnetite nanoparticles (NPs) have been converted into hydrophilic form using tetramethylammonium hydroxide (TMAOH). The advantage of this controlled surface functionalization approach is that there is no microstructural and phase alteration due to the ligand exchange. A tentative mechanism has been proposed to explain the formation of water soluble Fe_3O_4 NPs. Surface characteristics of NPs were studied with the aid of X-ray photoelectron spectroscopy (XPS). The so prepared hydrophilic magnetite NPs possess extraordinary relaxivity and contrast property making them potential T_2 contrast agent in clinical MR imaging.

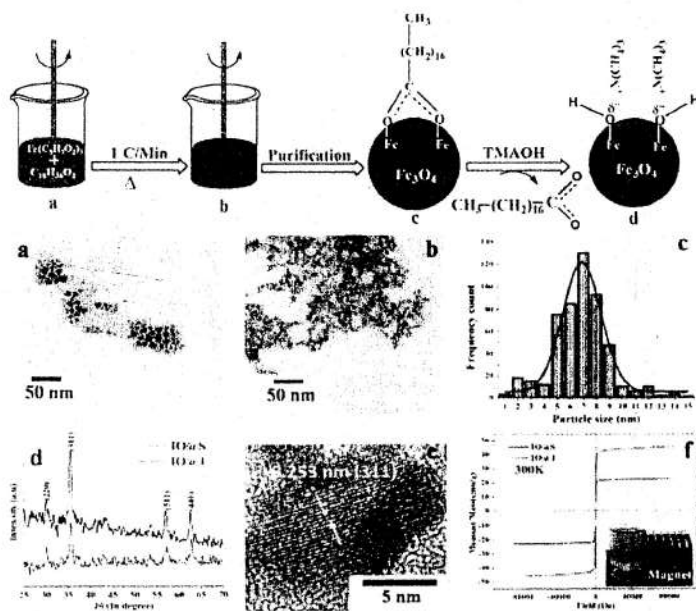


Figure 1 Schematic representation of synthesis and the consecutive ligand exchange of magnetite NPs, The TEM micrographs of IO@S and IO@T are shown in (a) and (b) respectively, (c) shows particle size distribution profile of IO@T NPs, (d) XRD pattern of the as-prepared and so-prepared magnetite NPs, (e) high resolution crystallographic image of IO@T, (f) hysteresis loop of the IO@T NPs at room temperature. The upper inset shows magnified view of the hysteresis loop while the lower inset shows nanoparticles behaviour under magnet.

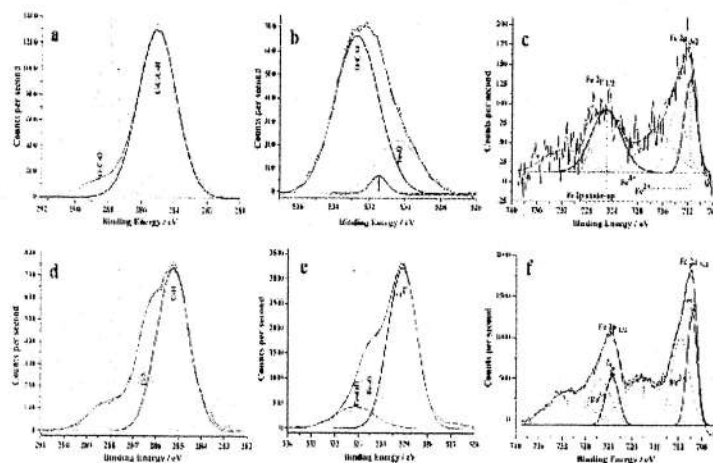


Figure 2 High resolution XPS spectra of magnetite NPs. The a, b, c and d, e, f are the C1s, O1s and Fe2p XPS spectra of IO@S and IO@T NPs respectively.

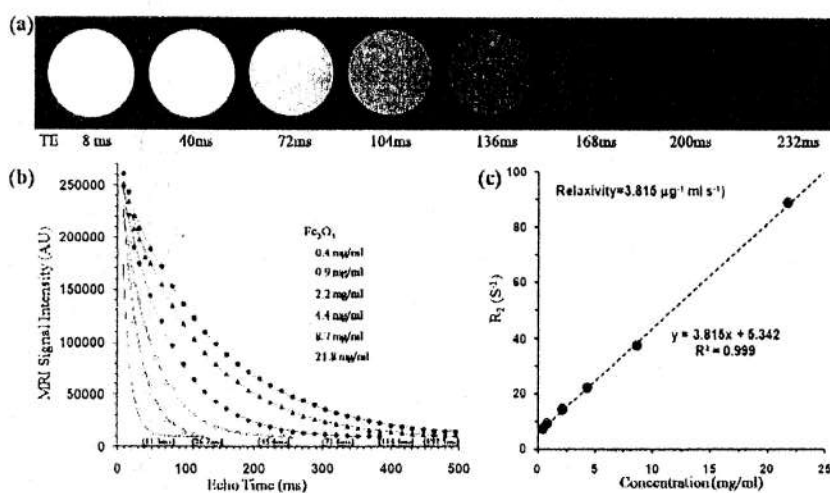


Figure 3 The transverse relaxivity of magnetite NPs. (a) The axial image of microfuge tube filled with magnetite solution (2 mg/ml), (b) the variation of MRI signal intensity with echo time at different concentration of magnetite NPs. Numbers in parenthesis below each curve represent the T_2 value, and (c) variation of transverse relaxation rate (R_2) with concentration of magnetite NPs. The slope indicates the relaxivity of the magnetite.

Conclusion: A facile, one-pot and open environment thermal decomposition method has been developed to fabricate monodispersed Fe_3O_4 NPs. A controlled ligand exchange based surface functionalization on hydrophilic NPs yields water soluble magnetite NPs. This direct monophasic replacement of fatty acid by TMAOH on the surface of NPs does not lead to any notable change in the microstructure and property. Moreover, a remarkable improvement in relaxivity has been obtained for the so prepared water dispensable magnetite NPs.

2.3 High luminescence biocompatible multimodal ZnSe(S) nanodots for biomedical applications

Abstract

Highly luminescent, non-heavy metal, multimodal alloyed nanodots (MAND) were developed for fluorescence imaging and sensing of biological systems. The synthesis parameters were optimized varying the precursor ratios, surfactant concentrations and the preparative pH, to achieve high performance, biocompatible ZnSe(S) MANDs with multimodal capabilities. The ZnSe(S) MANDs exhibited significant enhancement in their quantum yield (~30 %) compared to conventional ZnSe based systems, while retaining its biocompatibility characteristics. The multimodality of ZnSe(S) MANDs was shown by its capability of fluorescence imaging of cells and pH sensing abilities. The photoluminescence of MANDs shows prominent pH dependent modulation, in buffered suspensions of mammalian lymphocyte cells, over a wide pH range of 4.0-12.0. These endowments make the ZnSe(S) MANDs a novel system for development of cell tracking, monitoring and sensing intracellular nano probes and devices.

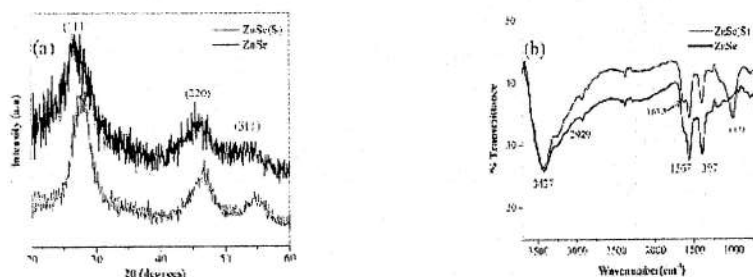


Figure 1. Comparative study of the ZnSe and ZnSe(S) systems using (a) XRD and (b) FTIR

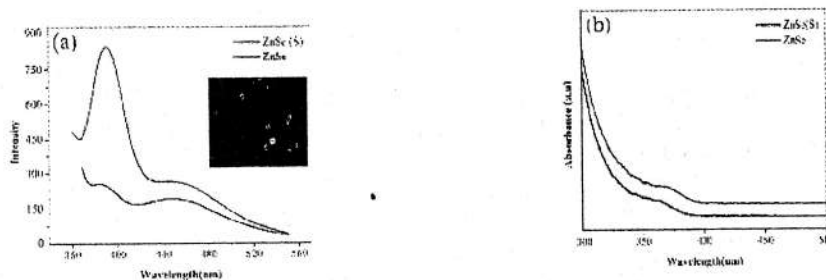


Figure 2. Optical property study of the ZnSe and ZnSe(S) systems using (a) PL and (b) UV-vis spectroscopy. The inset in (a) shows the fluorescence of ZnSe(S) nanodots clusters at 1000X magnifications.

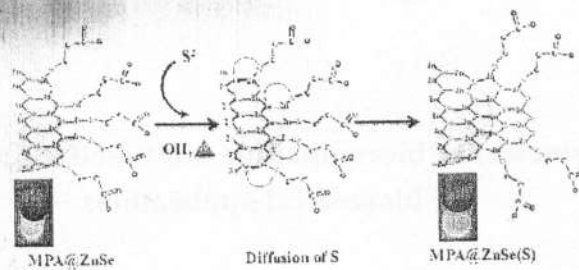


Figure 3. Schematic representation of the development of ZnSe(S) MAND. The inset shows the sample photographs under UV-light illumination.

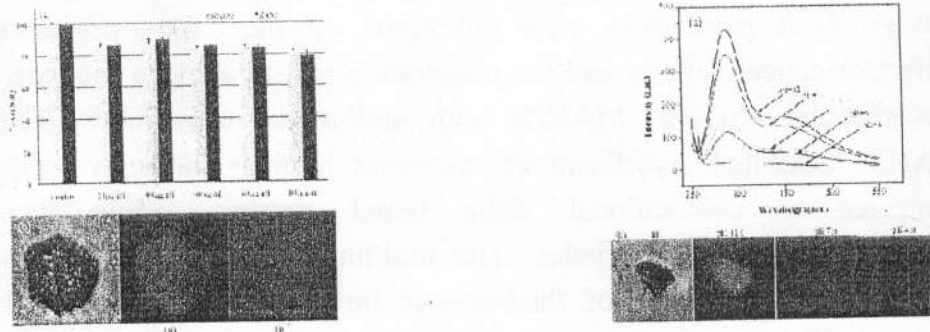


Figure 4. (a) MTT based cytotoxicity assay of the ZnSe and ZnSe(S) nanodots systems. (b) Uptake of ZnSe(S) MANDs by cultured lymphocytes at 630 X magnification, under (i) Bright field (ii) fluorescent ($\lambda_{\text{excitonic}} = 450 \text{ nm}$) and (iii) overlaid modes.

Figure 5(a) Effect of Ph variation on the PL spectra ZnSe(S) MAND. (b) Representative pictographs of the effect of Ph environment variation on fixed lymphocytes incorporated with ZnSe(S) MANDs. The bright field (BF) and fluorescent micrographs were obtained at 400x magnification.

Conclusion: In summary, ZnSe(S) MANDs were developed by optimizing the synthesis parameters to obtain a quantum yield of ~ 30%, which is an appreciable enhancement over the reported ZnSe systems. This enhancement can be attributed to the coincident Ostwald ripening and surface passivation resulting in the alloyed structure of ZnSe(S) nanodots. The surface passivation of sulphur resulting in the formation of ZnSe(S) MANDs also contributes to the chemical stability and hence biocompatibility. These attributes were confirmed from the high uptake in cells as well as low cytotoxicity in mammalian leukocytes cultures. The multimodal characteristics were manifested in the form of its application for fluorescence imaging and pH dependent *in vitro* fluorescence sensing. MANDs have a wide scope of futuristic applications, as a new class of multimodal fluorescent probes and/or sensors.

2.4 Differential tunability effect on the optical properties of doped and undoped quantum dots

Abstract

We have studied the optical properties of size-tunable undoped and Mn^{2+} -doped cadmium telluride (CdTe) quantum dots (QDs) of monodisperse suspensions with emission wavelength varying between 500 and 680nm. The role of the surface is investigated for obtaining size-tunable, bright, and stable CdTe QDs. Differentially tunable optical properties of doped and undoped CdTe QDs has been reported. Unlike the continuous red shifting in the absorption spectra of pristine CdTe system, an unusual blue shift is observed for doped CdTe system after a certain time period of refluxion, followed by again a red shift and the disappearance of earlier peak with further refluxing. The available size range and optical properties are significantly controlled through Mn^{2+} doping. The surface adsorbed Mn promotes ripening of the doped system as well as disintegration into smaller fraction after saturation in growth occurs. An optimum size fraction is identified for both the systems based on their photoluminescence (PL) quantum yield. The photophysics of Mn^{2+} -doped nanocrystals has been proposed.

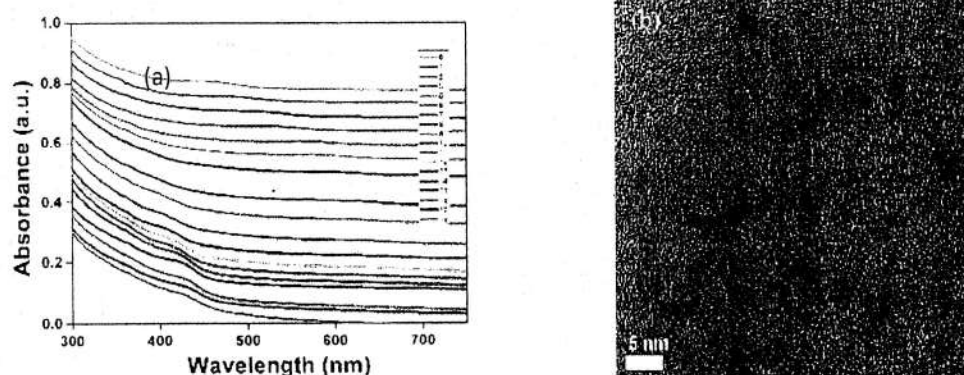


Figure 1 (a) UV Visible absorption spectra of Mn:CdTe QD & (b) HRTEM image of Mn:CdTe QD

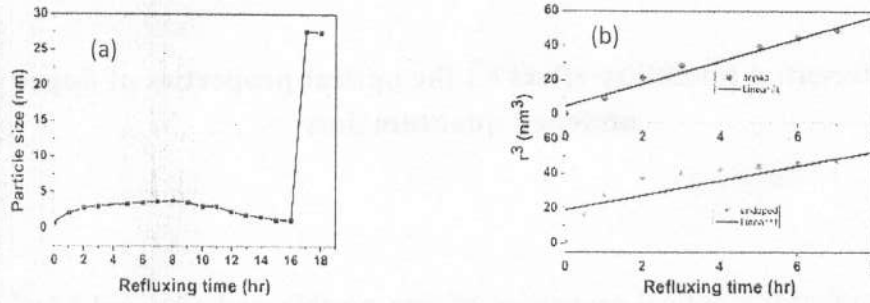


Figure 2 (a) Estimated particle sizes and (b) LSW plot of Mn:CdTe QD with refluxing time variation.

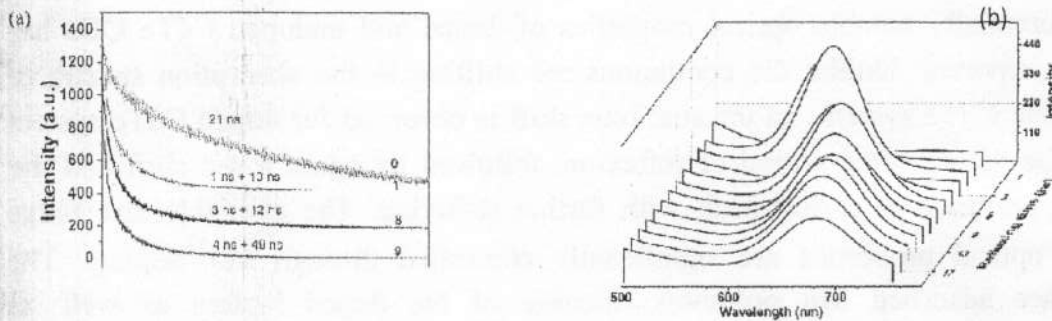


Figure 3 (a) TRPL spectra, (b) PL spectra of Mn:CdTe QD

Conclusion: In summary, an in-depth study on controlled tunability and understanding the mechanism has been carried out on undoped and doped CdTe QDs. We find that the size fraction of pristine CdTe formed at the equilibrium of growth and dissolution process possesses the high luminescence efficiency at room temperature. The same size fraction exhibiting luminescence enhancement on photoetching, smallest stoke's shift and minimum non-radiative decay rate correlates to their prior better quality surface. On doping Mn^{2+} with this CdTe QDs, the photo-luminescence emission of the d-dots can be controllably tuned in a narrow optical window. Time-resolved PL measurement show extremely short lifetime confirming emission due to surface adsorbed Mn^{2+} states. Moreover, doping has caused self assembly of the d dots in the form of pearl necklace microstructure which is due to antiferro-magnetic superexchange interaction between surface adsorbed species.

2.5 Direct monophasic replacement of fatty acid by DMSA on SPION surface

Abstract

Tailoring the surface and understanding the surface characteristics is necessary for biomedical applications of superparamagnetic nanoparticles. In this paper, superparamagnetic iron oxide nanoparticles (SPIONs) were prepared by thermal decomposition of iron nitrate in presence of stearic acid as surfactant. Due to the multilayer organization of surfactant molecules over the nanoparticle surface, the surface potential can be tuned by pH changes and hence the nanoparticles can be made dispersible in nonpolar as well as in polar solvents. We have presented a simple, facile procedure for controlled replacement of stearic acid from maghemite surface and subsequent derivatization by biocompatible dimercaptosuccinic acid (DMSA) to obtain ultrastable hydrophilic nanoparticles with unaltered morphology, phase and properties. The surface chemistry of the functionalized SPIONs was analyzed by Fourier transform infrared spectroscopy (FTIR), thermogravimetric analysis (TGA) and X-ray photoelectron spectroscopy (XPS) revealing the presence of bound and unbound thiol groups and disulfides, leading to its prolonged stability in aqueous medium. The consequence of spatially selective functionalization on the stability and solubility of surface hydrophilic SPION has also been realized.

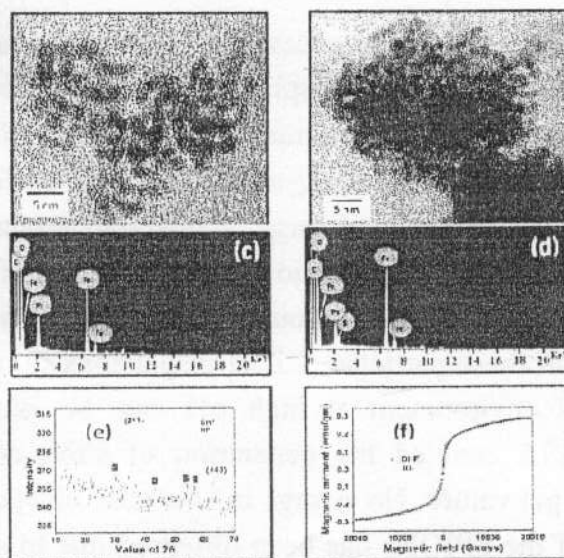


Figure 1 (a) and (c) show the HRTEM photograph and EDX pattern of stearic acid coated (HF) SPION while (b) and (d) show the same for DMSA functionalized (DHF) SPIONs respectively. The XRD pattern and magnetic characterization of both SPIONs are shown in (e) and (f) respectively.

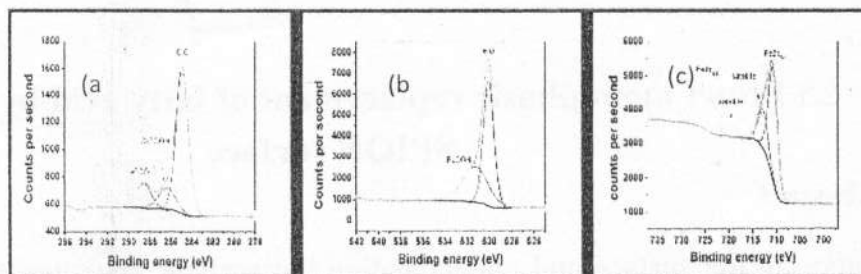


Figure 2 High resolution XP spectra of HF sample on Si wafer in (a) C1s, (b) O1s and (c) Fe2p regions

Figure 3 FTIR spectra of (a) HF sample at pH 3 and 11 and (b) HF and DHF samples. The inset of (a) shows the enlarged plot of the two samples in the wavenumber range 1800-1200 cm^{-1} .

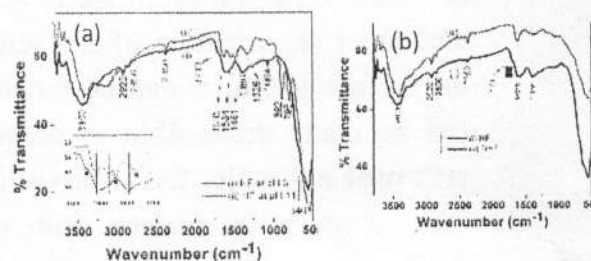
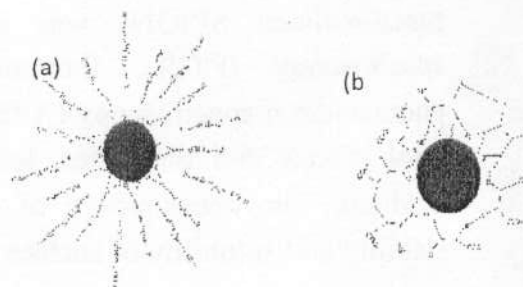


Figure 4 Schematic diagram of (a) Multilayer coating of stearic acids on SPION surface and (c) DMSA functionalization over SPION surface.



Conclusion: In this paper, we described a facile process for obtaining ultrastable surface hydrophilic SPIONs through controlled displacement of stearic acid by DMSA without any alteration in particle microstructure. Ultrafine SPIONs with average diameter of $\sim 3\text{nm}$ were synthesized using stearic acid as surfactant. The resulting particles have a thick shell of organic material around the inorganic part, which implies that the stearic acid coating consists of more than one layer. Presence of strongly and weakly bound stearic acid layers over SPION surface is evidenced. With these particles, stable dispersions in organic solvents as well as in aqueous environment at high pH can be obtained. Controlled replacement by DMSA enabled the generation of stable aqueous dispersions over a wide range of pH values. No change in the size, crystallinity, phase and magnetic behaviour of the SPIONs has been observed due to surface modifications.

2.6 Simple synthesis of superparamagnetic magnetite nanoparticles as highly efficient contrast agent

Abstract

Magnetite nanoparticles have been prepared by one-pot thermal decomposition process using iron (III) acetylacetonate in stearic acid in ambient environment. In this process, stearic acid acts as solvent as well as capping agent for the particles. These as-prepared hydrophobic magnetite nanoparticles have been converted into a hydrophilic form using tetramethylammonium hydroxide. This controlled surface functionalization approach limits microstructural and phase alteration due to the ligand exchange. A detailed investigation was carried out on the microstructural characteristics of these nanoparticles with the aid of X-ray diffraction, infrared spectroscopy, XPS and transmission electron microscopy. The hydrophilic superparamagnetic magnetite particles possess extraordinary transverse relaxivity and contrast property, making them potential T2 contrast agent in clinical magnetic resonance imaging.

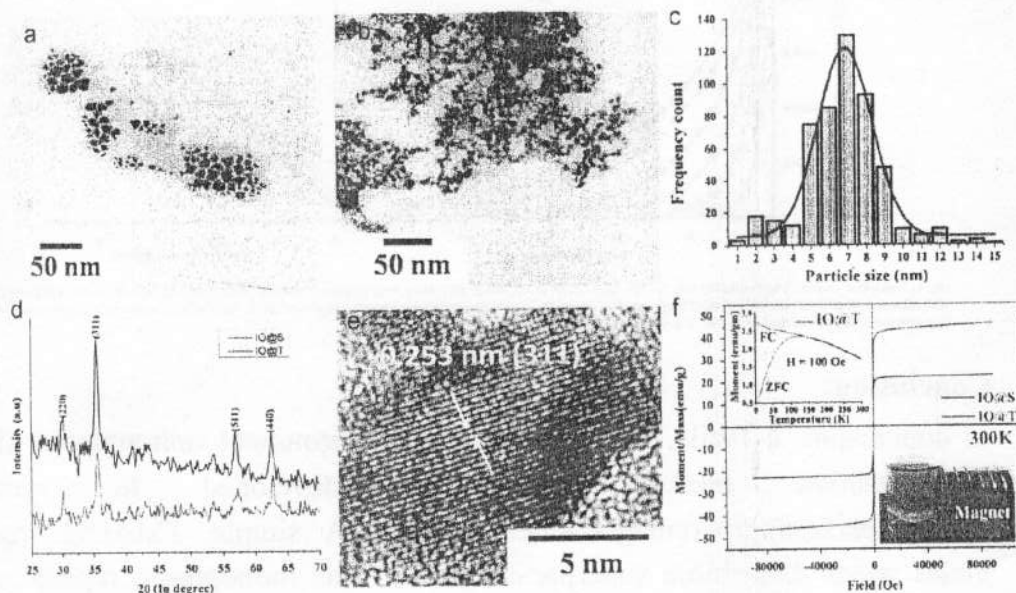


Fig. 1. TEM micrographs of IO@S and IO@T are shown in (a) and (b), respectively, while (c) shows particle size distribution profile of IO@T NPs. (d) XRD pattern of IO@S and IO@T. (e) high resolution TEM image of IO@T NPs and (f) magnetic hysteresis loop of IO@S and IO@T NPs at room temperature. Left upper inset shows magnetic moment vs temperature for zero field cooling (ZFC) and field cooling (FC) of IO@T sample. The right lower inset shows IO@T NPs behavior under magnetic field.

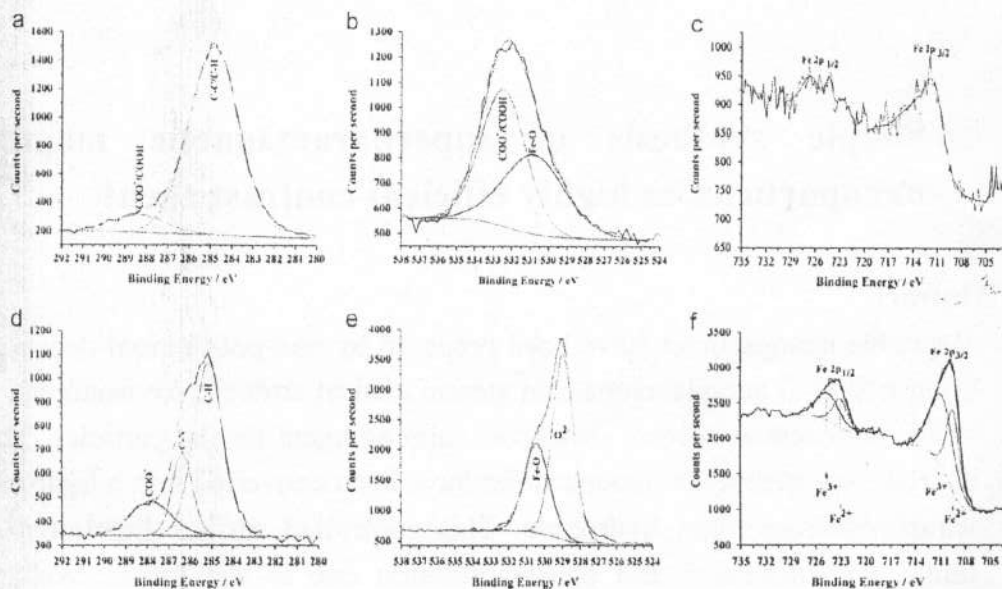


Fig. 2. High resolution XPS spectra of magnetite NPs. The a, b, c (IO@S) and d, e, f (IO@T) are the C1s, O1s and Fe2p spectra, respectively.

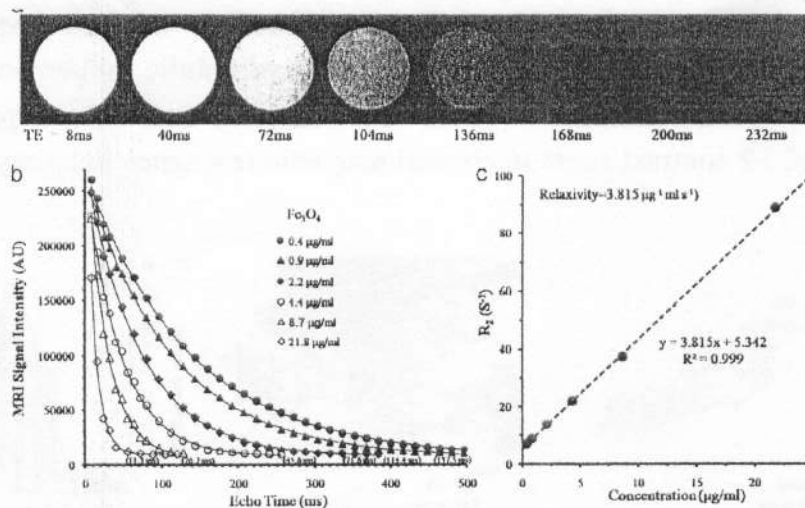


Fig. 3. Transverse relaxivity of magnetite NPs. (a) The axial image of microtuge tube filled with magnetite solution (0.9 µg/ml), (b) the variation of MRI signal intensity with echo time at different concentration of magnetite NPs. Numbers in parenthesis below each curve represent the T_2 value and (c) variation of transverse relaxation rate (R_2) with concentration of magnetite NPs. The slope indicates the relaxivity of the magnetite.

Conclusion:

In conclusion, a facile, one-pot and open environment non-aqueous thermal decomposition method has been developed to synthesize monodispersesuperparamagnetic Fe_3O_4 NPs. A simple TMAOH treatment yields water dispersible superparamagnetic. This monophasic replacement of fatty acid by TMAOH on the surface of NPs does not lead to any notable change in the microstructure and phase. A high transverse relaxivity of obtained magnetite NPs has been observed for MRI contrast application.

2.7 Enhanced Quantum Confined Stark Effect in a Mesoporous hybrid multifunctional system

Abstract

Quantum Confined Stark Effect in hybrid of CdTe quantum dot with superparamagnetic iron oxide nanoparticles in both nonporous and mesoporous silica matrix has been realized. The observed QCSE is due to the local electric field induced by charge dispersion at SiO₂/polar solvent interface. Enhanced Stark shift of 89.5 meV is observed in case of mesoporous hybrid structure and the corresponding local electric field has been evaluated as 4.38×10^4 V/cm. The enhancement is assumed to be caused by greater density of charge in the mesoporous hybrid. The conjugation of superparamagnetic nanoparticles in this tailored hybrid microstructure has not imparted any alteration to the Stark shift, but has added multifunctional attribute. The present study on the local electric field induced enhanced QCSE with wavelength modulation towards red end paves the way of developing magneto-fluorescent hybrid systems for biomedical imaging application.

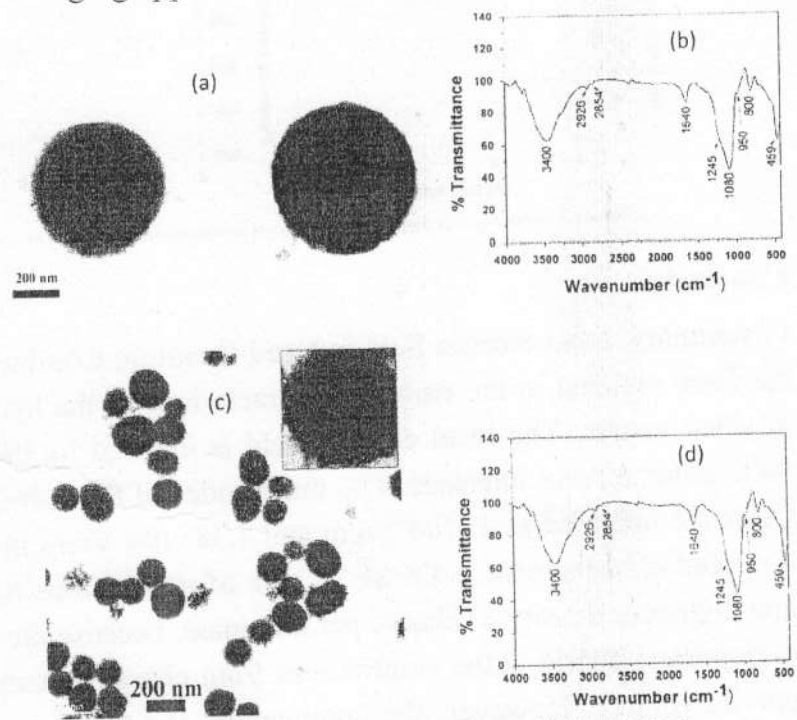


Fig. 1. HR-TEM image of (a) hybrid A, (c) hybrid B and FTIR spectra of (b) hybrid A (d) hybrid B.

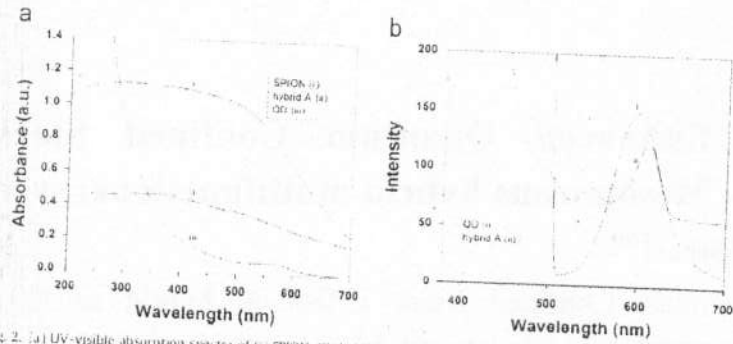


Fig. 2. (a) UV-visible absorption spectra of (i) SPION, (ii) hybrid A and (iii) QD, and (b) PL spectra of (i) QD and (ii) hybrid A.

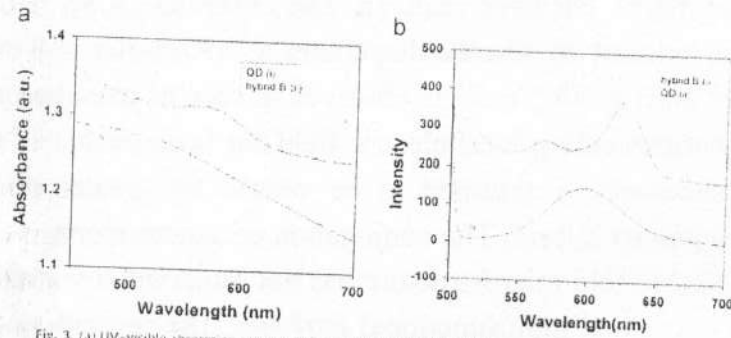


Fig. 3. (a) UV-visible absorption spectra of (i) QD and (ii) hybrid B, (b) PL spectra of (i) hybrid B and (ii) QD.

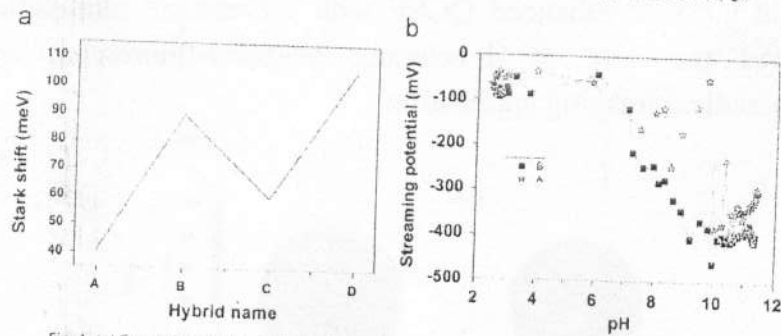


Fig. 4. (a) Comparative Stark shift in hybrid samples and (b) streaming potential plot of hybrids A and B.

Conclusion:

In summary, local electric field induced Quantum Confined Stark Effect (QCSE) has been realized in the emission characteristic of the hybrid of QD and SPION in silica matrix. The local electric field is induced by the charge dispersion on SiO₂/polar solvent interface. The magnitudes of the corresponding local electric fields are obtained as 2×10^4 V/cm and 4.38×10^4 V/cm in hybrids A and B. The observed enhancement in QCSE in case of mesoporous hybrid is assumed to be due to greater density of charge per unit mass, because the total charge density of mesoporous hybrid is the contribution from charge density on outer surface and porous volume. However, the conjugation of SPION to the hybrid to achieve multifunctional attribute has no influence on the observed QCSE. Such a magneto-fluorescent hybrid system with emission wavelength modulation towards red end has potential in biomedical imaging.

2.8 Sensitive fluorescence response of ZnSe(S) quantum dots: an efficient fluorescence probe

An efficient fluorescence probe based on ZnSe(S) alloyed quantum dots (QDs) has been reported here. The alloyed QDs were prepared through an aqueous route, where 3-mercaptopropionic acid (MPA) was employed as the effective precursor for both the sulfur source and stabilizer in the development of the alloyed system. Five-fold quantum yield (QY) enhancement was obtained for the ZnSe(S) QDs compared to the ZnSe QDs, formed in the initial stage of the refluxing process. The ultimate alloyed systems retained their high biocompatibility characteristics similar to the conventional ZnSe QDs. The photoluminescence of the ZnSe(S) QDs showed pH dependence, which was also evidenced in mammalian lymphocyte cells suspended in biological buffer over a wide pH range of 4.00–12.00. These characteristics make our prepared ZnSe(S) an efficient system for development of cell tracking, monitoring and sensing intracellular

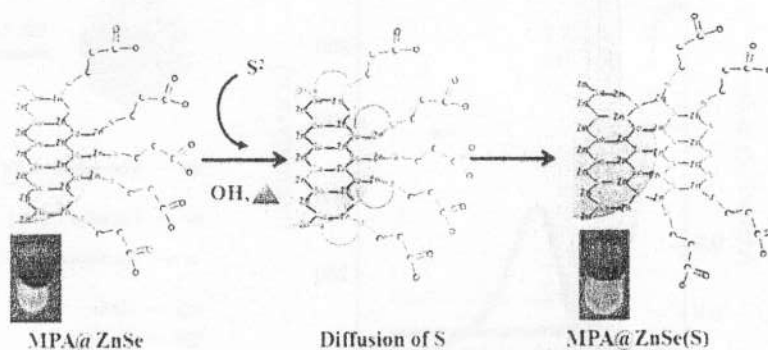


Fig. FTIR spectra of MPA-capped ZnSe and ZnSe(S) QDs. (b) Schematic mechanism of ZnSe(S) alloy formation. The inset shows the sample photographs under UV-light illumination.

Conclusion

In summary, ZnSe(S) QDs were developed with QYs of ~55%, which is an appreciable enhancement over the reported ZnSe systems. This enhancement can be attributed to the coincident Ostwald ripening and surface passivation resulting in the alloyed structure of ZnSe(S) QDs. The surface passivation of sulfur resulting in the formation of ZnSe(S) QDs also contributes to the chemical stability and hence biocompatibility. These attributes were confirmed by the high uptake in cells as well as the low cytotoxicity in mammalian leukocyte cultures. The capability of the fluorescence probe was manifested in the form of its application for fluorescence imaging and pH-dependent *in vitro* fluorescence sensing.

2.9 Significant improvement in dopant emission and lifetime in water soluble Cu:ZnSe/ZnS nanocrystals

We report here the enhanced dopant emission in Cu:ZnSe/ZnS core-shell nanocrystals (NCs) through an aqueous route in ambient conditions. A three-fold quantum enhancement in luminescence has been achieved by developing a ZnS inert shell as compared to the pristine doped NCs. The internal doping of Cu after shell growth, signifying localization of Cu²⁺ t₂ energy states in the deep band gap, has shown a significant improvement in dopant excited state lifetime. The long lifetime related to Cu dopant emission is the longest lifetime ever reported for copper doped zinc based NCs developed through an aqueous route. The good colloidal as well as the luminescence stability of these highly efficient doped NCs mean they have great potential for use in biomedical imaging applications.

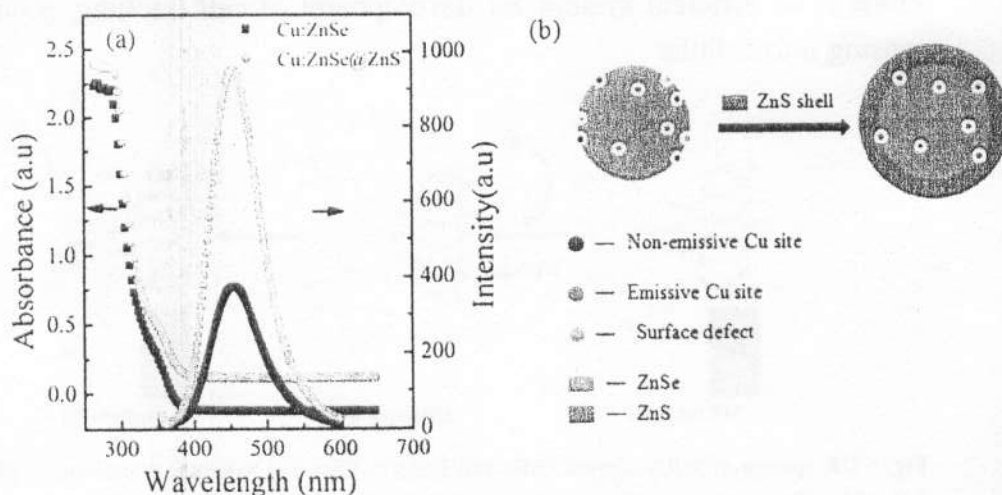


Figure 2. (a) UV-visible absorption and PL spectra of Cu:ZnSe NCs and Cu:ZnSe/ZnS NCs, (b) schematic of ZnS surface passivation of Cu:ZnSe NCs.

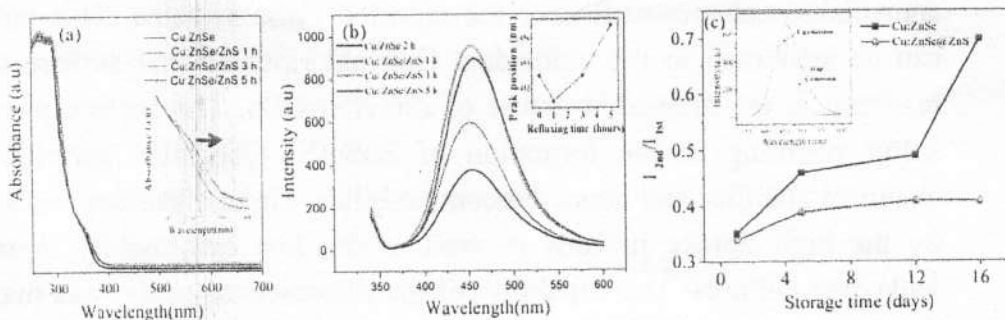


Figure 2. (a) UV-visible of Cu: ZnSe and Cu:ZnSe/ZnS NCs with different refluxing intervals, (inset shows the red shifting of absorption peak), (b) PL spectra of Cu:ZnSe and Cu:ZnSe/ZnS NCs with different refluxing intervals (inset shows the peak positions against the refluxing time) and (c) I2nd /I1st plot against the storage times of both NCs (inset shows deconvolution of PL spectra).

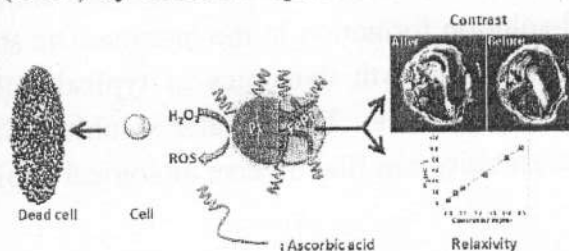
Conclusion

In summary, we have developed highly luminescent blue-emitting Cu doped Zn based NCs through an aqueous route and demonstrated that the Cu²⁺ emissive centers in Cu doped ZnSe NCs can be optically activated by developing a ZnS inert shell matrix. As compared to the copper doped ZnSe NCs the doped core-shell NCs have shown three-fold PL QY enhancement. The significant increment of Cu dopant excited states lifetime after ZnS shell formation implies that the Cu²⁺ states are localized deep in the optical band gap avoiding unwanted overlapping with the surface trap states. This gives the essence of the internal doping of Cu to the ZnSe host possible through our simple aqueous route. The interfacial solid-solution formation in the intermediate stage of shell growth gives an insight into the growth dynamics of typical semiconductor core-shell NCs using this aqueous route. These water soluble NCs with high PL efficiency and long term stability can find diverse biological applications.

2.10 Single moiety, multifunctional iron-platinum nanoparticles for potential MR imaging and therapeutic applications

Abstract:

We have reported a one-step, green chemical route for synthesis of iron platinum nanocomposite (Pt-FePt) which consists of cubic Pt and FePt phases. These nanosystems have been studied thoroughly for microstructural, compositional and magnetic property and optimized for biomedical applications. Superior relaxivity and contrast property has been obtained in mice model with optimized nanoparticle concentration. Consequent catalytic efficiency of Pt of the nanocomposite has been explored for therapeutic application. We have observed that Pt could catalyze decomposition of H_2O_2 into reactive oxygen species (ROS) at neutral pH which are cytotoxic. This has the potential of causing cellular damage and cell death of targeted tumour cells. The H_2O_2 decomposition vs. nanoparticle concentration is monitored by adding a dye, dichlorofluorescein (DCFH), which is converted to its fluorescent form dichlorofluorescein (DCF) by the ROS species.



Scheme 1. Schematic depiction of Pt-FePt nanocomposite for imaging and therapeutic applications

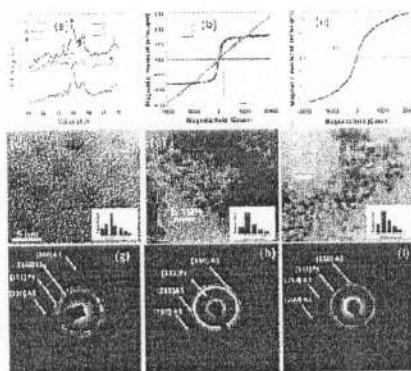


Figure 1(a) XRD patterns of three samples. Figure 1(b) Magnetization curve of P1, P3 and only Pt nanoparticles. The inset shows the enlarged magnetization curve of P1 sample near origin and (c) Magnetization curve of P2 sample. Figure (d), (e), (f), (g), (h) and (i) show the HRTEM images and SAD pattern analysis of P1, P2 and P3 samples, respectively. The insets of Figure (d), (e) and (f) show the size distribution histograms of the nanoparticles.

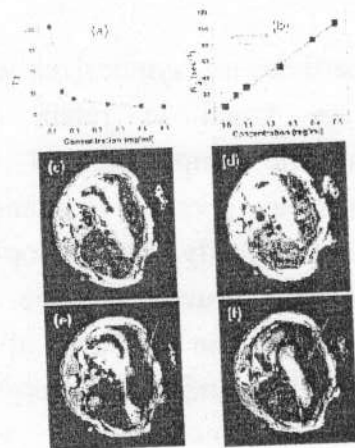


Figure 2 (a) Transverse relaxation time (T2) and (b) Transverse relaxation rate (R2=1/T2) with varying concentration of P2. The slope of the line in panel b indicates the relaxivity. The T2 weighted MR images of mouse abdomen pre (c and d) and post administration of P2. The hypointensity in liver following administration of P2 is marked with red arrow (e, f).

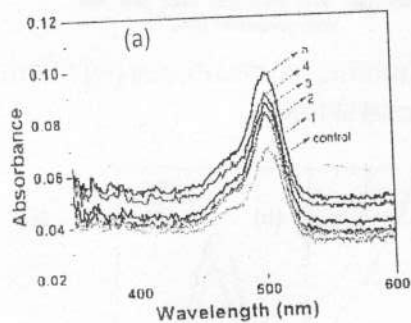


Figure 4 (a) Decomposition of H_2O_2 using P2 sample indicated by increasing absorbance of ROS sensitive DCF. Here sample 1,2,3,4 and 5 are designated by the amount of P2 used as 50 μ L, 100 μ L, 150 μ L, 200 μ L and 250 μ L of a solution of concentration 1 mg/ml. Figure 3(b) and (c) show the fluorescence micrographs of control and sample 5.

Conclusion: In summary, we have developed a superparamagnetic iron platinum nanocomposite system with synergistic enhancement in MR contrast. The nanocomposite system was tested as efficient therapeutic agent based on its excellent catalytic property. The concept of single moiety, multifunctional nanosystem developed through a simple, green chemical route can cater the platform technology for simultaneous imaging and diagnosis of diseased cells.

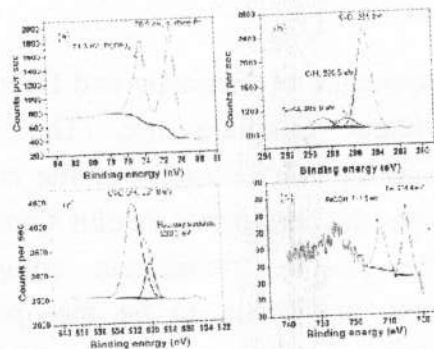
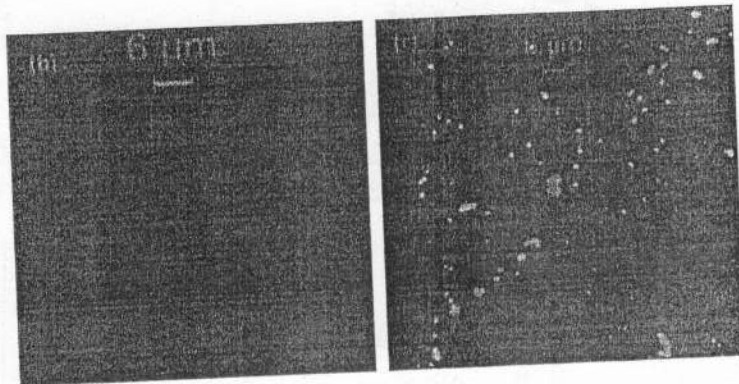


Figure 3 XPS spectra of (a) Pt 4f7/2 and Pt 4f5/2, (b) C1s, (c) O1s and (d) Fe 2p peaks for P2 sample.



2.11 Hierarchically architected multifunctional mesoporous maglumino hybrids

Abstract

Silica conjugate of magnetic and fluorescent nanoparticles are synthesized with and without template use. The conjugates are found to retain the superparamagnetic character of the constituent magnetic component. At the same time, the conjugates exhibit fluorescence without any decrease in intensity than the pristine fluorescent component. Morphologically, the template conjugates are found to be mesoporous, hollow like structures while the untemplated ones are seem to be solid spherical particles. The efficiency of the conjugates for biomedical applications is checked by BSA and drug adsorption experiments. Prior to drug loading the conjugates are functionalized with APTES. Then both protein and drug are assumed to be adsorbed over conjugate surfaces through electrostatic force of attraction between oppositely charged species.

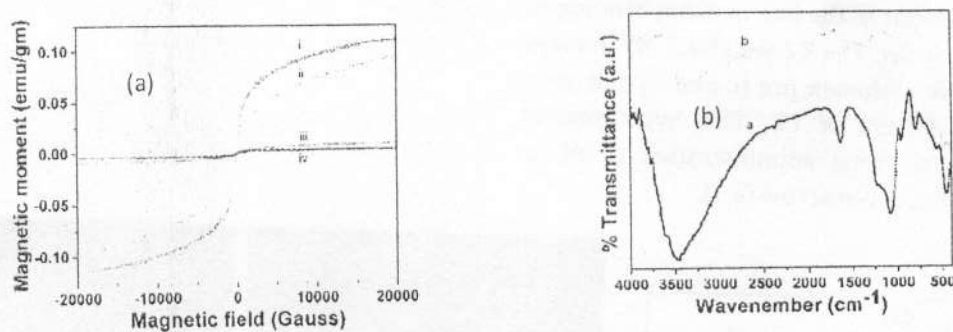


Figure 1 (a) VSM curves of (i) iron oxide nanoparticles, (ii) NK8HC, (iii) NK1HC and (iv) NK9HC samples and (b) FTIR spectra of (a) NK1HC and (b) stearic acid@SPION.

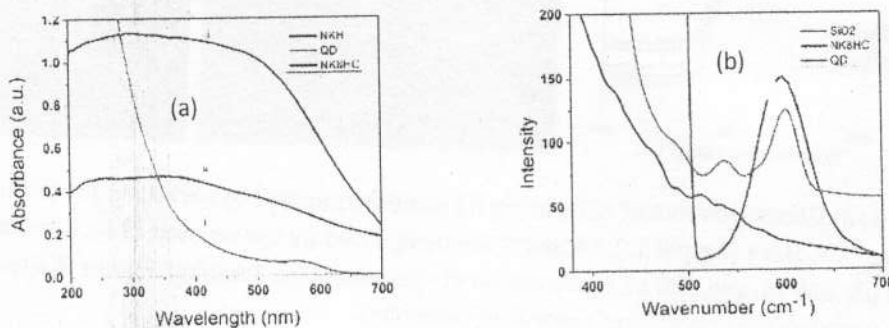


Figure 2 (a) UV-visible absorption spectra of i. MSA@CdTe QD, ii. NK8HC and iii. SPION and (b) PL plot of MSA@CdTe QD, SiO₂ and NK8HC sample

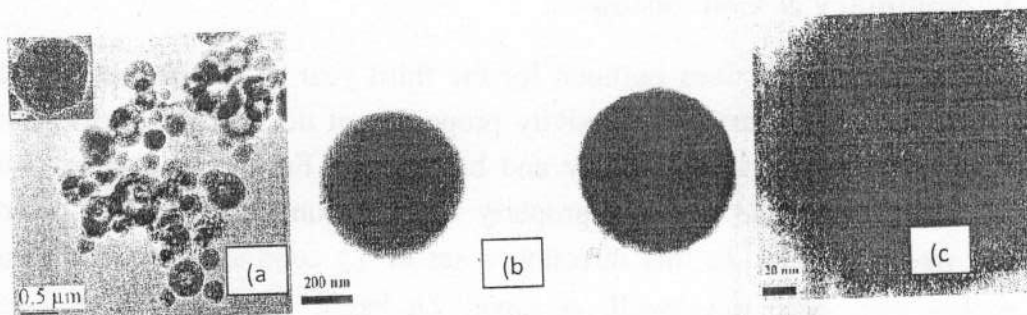


Figure 3 HRTEM images of (a) NK1HC, (b) NK8HC and (c) NK9HC samples.

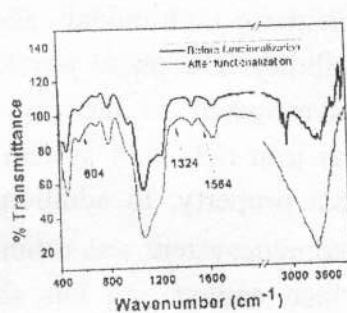


Figure 4 Comparative FTIR spectra of silica conjugate before and after APTES functionalization.

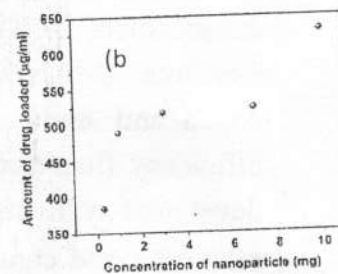
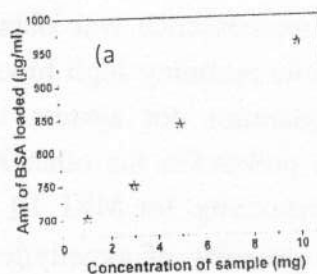


Figure 5 (a) BSA adsorption on silica conjugate nanoparticles and (b) Aspirin loading on silica conjugate nanoparticles.

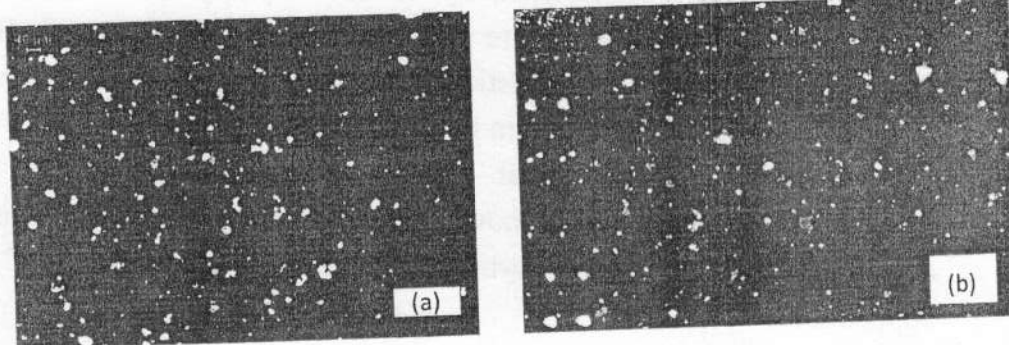


Figure 6 Fluorescence images (a) NK8HC and (b) NK9HC samples.

Conclusion: In summary, we have reported hollow mesoporous silica beads entrapping stearic acid stabilized magnetite (Fe_3O_4) nanoparticles using CTAB. Also, DMSA modified magnetite (Fe_3O_4) nanoparticles and MSA stabilized CdTe quantum dots are simultaneously encapsulated with and without any mesoporous structure of silica nanoparticles. The developed hybrid nanosystems exhibit magnetic-fluorescent properties and protein loading capability hence multifunctionality is achieved with system. Further, the hybrid nanoparticles are functionalized with APTES molecules and used for drug loading purpose.

3. Summary & Conclusion

The scientific objectives outlined for the third year of the project included the evaluation of contrast and relaxivity properties of developed hybrid nanosystem along with their biocompatibility and biostability. Further, it also involved the characterization and contrast property optimisation of the hybrid nanosystem and its constituents. In this direction a set of T₂ contrast agent and fluorescent probes have been developed. A novel Zn based nontoxic fluorescent probes was developed with potential multimodal applications in imaging and sensing. The role of surfactant in controlling their emission was revealed. A significant enhancement in photoluminescence was obtained in these multimodal alloyed nanodots (MAND) while retaining high biocompatibility. The photo physics of doped and undoped quantum dot system was investigated to identify high efficiency fluorescence probes. On the other hand an iron rich FePt system was developed with high relaxivity for MRI T₂ contrast property. In addition, the relaxivity and contrast property of already developed nanosystem was estimated. Interestingly this iron oxide system after surface engineering has shown superior aqueous dispersibility, stability and relaxivity. Then a novel magneto-fluorescent hybrid nanosystem was developed with the aforementioned components. The multifunctionality of this nanosystem was engineered by developing mesoporous structure in the host matrix with controlled functionality. The multifunctional characteristics - magnetic imaging, fluorescence imaging, drug loading and targeted protein binding - were evaluated. The development of a single moiety multifunctional hybrid nanosystem integrating imaging and therapeutic properties was a novel outcome in this direction. This system was developed through a green synthesis route keeping in mind of its potential applications.

4. Details of New Leads Obtained

The integration of imaging and therapeutic property in single moiety multifunctional hybrid nanosystem is unique and the patent has been applied on this concept, which can be extended to other hybrid nanosystems. Two more patent have already been applied on the discoveries of a method for microstructural analysis and a method for kinetic analysis of nanomaterials respectively. These methods are useful for analysing bulk materials also. Development of a multifunctional hybrid nanosystem capable of executing fluorescence imaging, magnetic imaging, drug delivery and targeted protein

binding is a unique outcome of the project. The new leads in terms of developing few T2 contrast agents and fluorescent probes alongwith the underlying science behind achieving unusual efficiency are the important achievement of the project. All these individual studies were published in reputed international journals and some of the studies are already communicated for publication.

5. Outcomes of the project

Papers published in refereed journals

International

1. Deepak K Jha, P. Deb, E. Kalita, M. Shameem and Anant B Patel "Synthesis and characterization of iron rich $\text{Fe}_x\text{Pt}_{1-x}$ ferrofluid for magnetic resonance imaging" Phys. Scr. 85, 2012, 035802-07.
2. S Chakraborty, M Gogoi, E Kalita and P Deb "Multifunctional, high luminescent, biocompatible CdTe quantum dot fluorophores for bioimaging applications" Int. J. Nanoscience 10, 2011, 1191-1195
3. K Saikia, P Deb, E Kalita, Facile synthesis of highly luminescent ZnSe(S) alloyed quantum dot for biomedical imaging Current Applied Physics 13 (2013) 925-930
4. M Gogoi, P Deb and A Kostka "Differential tunability effect on the optical properties of doped and undoped quantum dots" Phys. Status Solidi A 209, 2012, 1543-1551
5. M Gogoi, P Deb, G Vasan, P. Keil, A. Kostka and A. Erbe "Direct monophasic replacement of fatty acid by DMSA on SPION surface" Applied Surface Science 258, 2012, 9685- 9691.
6. D K Jha, M Shameem, AB Patel, A Kostka, P Schneider, A Erbe, P Deb, Simple synthesis of superparamagnetic magnetite nanoparticles as highly efficient contrast agent, Materials Letters 95, 2013, 186-189.

7. M. Gogoi, P. Deb, D. Sen, S. Mazumder and A. Kostka, Enhanced Quantum Confined Stark Effect in a mesoporous hybrid multifunctional system, *Solid State Communication* 187 (2014) 48-52.
8. K Saikia, P Deb, E Kalita, Sensitive fluorescence response of ZnSe (S) quantum dots: an efficient fluorescence probe, *Phys. Scr.* 87 (2013) 065802.
9. K. Saikia, P. Deb, B. Mondal and E. Kalita, Significant improvement in dopant emission and lifetime in water soluble Cu: ZnSe/ZnS nanocrystals. *Materials Research Express* 1 (2014) 015014.
10. M. Gogoi, K. S. Varadragan, P. Schneider, G. Vasan, A. Kostka, A. Erbe, A. B. Patel, P. Deb, Magnetic property variation in iron platinum nanoparticles by simple route to develop theranostic agent, (accepted in *J. Mag. Mag. Mater.*).

National

1. P. Deb, E. Kalita, 2011, Development of biocompatible colloidal FePt nanoparticles for nanobiomedical applications using a green synthetic approach, *Journal of Assam Science Society*, 52 (2), 7-11
2. E. Kalita, P. Deb, 2012, Surface engineered biocompatible superparamagnetic iron oxide nanoparticles (SPIONS) as stable, colloidal dispersions for magnetic imaging applications, *Journal of Assam Science Society*, 53 (1), 12-16
3. P. Deb, K. Saikia, 2011, Opportunities and challenges in nanoelectronics and nanophotonics, *The Physics behind Electronics/ Optoelectronics and their application*, 1, 70-75

Papers communicated

1. M. Gogoi, D. Sen, S. Mazumder, P. Schneider, A. Erbe, A. Kostka, A. B. Patel and P. Deb, Hierarchically architected multifunctional mesoporous maglumino hybrids (under review)

Patents applied

1. A patent entitled "Method for kinetic analysis of solid state processes from nonisothermal calorimetry." is applied to Biotechnology Patent Facilitating Cell, DBT, Govt. of India (Application No.: BT/BPFC/04/70/2012)
2. A patent entitled "Multifunctional nanoparticles and methods for synthesis thereof" is applied to Biotechnology Patent Facilitating Cell, DBT, Govt. of India (Application No.: 1742/DEL/2013).

Software copyright awarded

The following softwares are developed and copyrighted

1. MaxQ – programme for microstructural study of nanomaterials from X-ray diffraction pattern analysis (SW-8076/2014)
2. KinLAC – programme for kinetic analysis of solid state processes (SW-8075/2014).

Conference Papers

1. A paper entitled "Engineered biocompatible superparamagnetic iron oxide nanoparticles " by M.Gogoi, D.K.Jha, R.Goswami, E. Kalita and P. Deb presented in the National Conference on Smart Nanostructures (NCSN-2011) held in Tezpur University (Central University) during 18-20th January, 2011.
2. Colour tunable ZnSe quantum dots synthesized by a novel method, D. Borgohain, D.K. Jha and P. Deb presented in National Workshop on Nuclear and Atomic Techniques based pure and applied sciences (NATPAS 2011) to be held in Tezpur University (Central University) during 1-3rd February, 2011.

3. Spectroscopic characterization of iron oxide nanoparticle functionalized through amide bond mediation, H. Medhi, M. Gogoi and P. Deb, presented in National Workshop on Nuclear and Atomic Techniques based pure and applied sciences (NATPAS 2011) to be held in Tezpur University (Central University) during 1-3rd February, 2011.
4. Silica encapsulation of magneto fluorescent conjugation and its Characterizations, K. Saikia, M. Gogoi and P. Deb, presented in National Workshop on Nuclear and Atomic Techniques based pure and applied sciences (NATPAS 2011) be held in Tezpur University (Central University) during 1-3rd February, 2011.
5. Superstructure formation in iron oxide nanoparticles studied through electron diffraction method, M Gogoi and P. Deb, in National Workshop on Nuclear and Atomic Techniques based pure and applied sciences (NATPAS 2011) to be held in Tezpur University (Central University) during 1-3rd February, 2011.
6. Spectroscopic study on the surface characterization of engineered FePt nanoparticles, D. K. Jha, E. Kalita and P. Deb, in National Workshop on Nuclear and Atomic Techniques based pure and applied sciences (NATPAS 2011) to be held in Tezpur University (Central University) during 1-3rd February, 2011.
7. Microstructural characterization of nanocrystals using XRD analysis techniques, S. Ahom and P. Deb, in National Workshop on Nuclear and Atomic Techniques based pure and applied sciences (NATPAS 2011) to be held in Tezpur University (Central University) during 1-3rd February, 2011.
8. A paper entitled "Opportunities and challenges in nanoelectronics and nanophotonics" by P. Deb and K. Saikia was published in the conference proceeding of the national conference "The physics behind electronics/Optoelectronics and Their applications" held in Sammilani

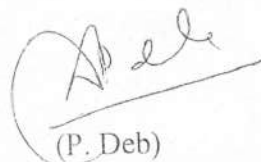
Mahavidyalaya, Kolkata during 1-2nd Dec 2011.

9. Multicolour, high luminescent, biocompatible CdTe quantum dot based fluorophores for bioimaging applications, S. Chakrabarty, M. Gogoi, E. Kalita and P. Deb presented in International conference on Nanoscience and Technology (ICONSAT 2010) held in IIT Mumbai during 18-20th February, 2010.
10. Surface Functionalization Mediated Enhanced Bio-distribution of Superparamagnetic Iron Oxide Nanoparticles (SPION) for Diagnostic Applications, H. Sonowal, M. Gogoi, E. Kalita, G. Vasan, A. Erbe and P. Deb, presented in International conference on Nanoscience and Technology (ICONSAT 2010) held in IIT Mumbai during 18-20th February, 2010.

6. Instruments Procured and Installed




Figure 1 (a) Atomic Force Microscope (AFM), (b) Physical Property Measurement System (PPMS), (c) Fluorescent Light Microscope (FLM), (d) pH Meter, (e) 40KV UPS, (f) Electronic Balance, (g) Tube Furnace, (h) ELISA Reader, (i) Laminar Air Flow, (LAF) (j) Centrifuge and Fridge (k) Hot Air Oven, (l) Deep Fridge, (m) Synthesis Lab, (n) Sophisticated Instrument Lab (o) Computational Facility and (p) Water Chiller.

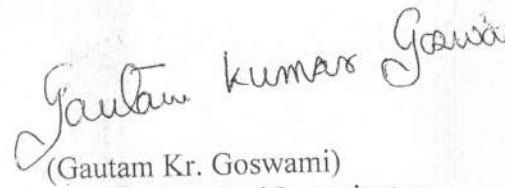


(P. Deb)
Principal Investigator,
Tezpur University (Central University)

Principal Investigator
"Multi Functional by brid.....
imaging applications."
DBT Project.
DEPARTMENT OF PHYSICS.
TEZPUR UNIVERSITY.

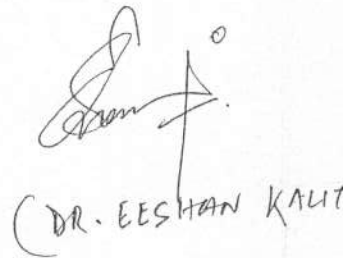


Dr. Dipu Bhuyan
Associate Professor
Dept. of Radiology
Gauhati Medical College



(Gautam Kr. Goswami)
Co-Principal Investigator
Gauhati Medical College Hospital

**Professor of Radiology,
Gauhati Medical College & Hospital
Guwahati-32.**



Dr. Eeshan Kalita
Asstt. Professor
Dept. of Molecular Biology & Biotech
Tezpur Central University

No. BT/PR10874/NNNT/28/136/2008 Dated. 6.2.2009

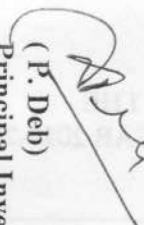
Utilization Certificate / Statement of Expenditure


Year 2009-12

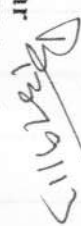
Recd. / Not /Recd.

Remarks

	Sanctioned cost	Actual cost	Balance	
Equipment	30727000.00	30727000.00	0.00	
Equipment procured without Sanction	Item	Cost	Amount to be reimbursement	
N/A	N/A	N/A	NIL	


 (P. Deb)
 Principal Investigator
 DBT Project
 Tezpur University


 Finance Officer
 Tezpur University
 OSD Finance
 Tezpur University


 Registrar
 Tezpur University
 Registrar
 Tezpur University

Principal Investigator
 "Multi Functional by bridging applications."
 DBT Project.
 DEPARTMENT OF PHYSICS,
 TEZPUR UNIVERSITY.

2012 June	0.00	16000.00	0.00
2013 July	0.00	16000.00	0.00

CONSOLIDATED STATEMENT FOR THE FINAL SETTLEMENT OF ACCOUNTS
 Sanction no. BT/PR/1087/4/NNTT/28136/2008 Dated: 6.2.2009

ITEM	Sanctioned outlay	Released fund by DBT		Expenditure as per latest statement of expenditure (SOE)					Balance as per released fund Rs.	Interest earned Rs.	Expenditure adjustment upto project end period 2012-13	Grand total expenditure	Remarks
		(pages)	(pages)	Rs.	(in lakh)	1st	2nd	3rd					
	Total Rs. (in lakh)	Total Rs. (in lakh)	Total Rs (in lakh)	9.2.2009 to 31.3.2009	1.4.2009 to 31.3.2010	1.4.2010 to 31.3.2011	1.4.2011 to 31.3.2012	1.4.2012 to 30.6.2012					
Equipment	307.27	307.27	0.00	31200.00	2120385.00	28183451.00	299894.00	92070.00	476469.00	3111399.00	Excess expenditure met from interest		
Manpower	9.82	3.10	0.00	135745.00	240000.00	(-144000.00)	0.00	78255.00	519200.00	750945.00			
Consumable	33.00	11.00	0.00	201031.00	886977.00	0.00	0.00	12992.00	862653.00	1949661.00			
Travel	1.50	0.50	0.00	95171.00	0.00	0.00	0.00	(-45171.00)	81287.00	176458.00	amount of Rs.		
Contingency	1.50	0.50	0.00	63442.00	1103.00	201.00	0.00	(-14746.00)	133269.00	198015.00	2122842/-		
Overhead	3.00	1.00	0.00	50000.00	0.00	0.00	0.00	50000.00	223364.00	273364.00	Balance		
Total	356.09	323.37	0.00	526589.00	3297465.00	28039652.00	299894.00	173400.00	2122842.00	2296242.00	34459842.00	NIL	

Fund released Rs. 32337000.00
 Interest earned Rs. 2122842.00
 Total Fund available Rs. 34459842.00
 Total expenditure Rs. 34459842.00
 Balance Rs. NIL

Release fund balance upto 30th June, 2012 Rs. 173400.00
 Total interest earned Rs. 2122842.00
 Total Fund available Rs. 2296242.00
 Total expenditure upto project end Rs. 2296242.00
 Balance Rs. NIL

(P. Deb)
 Principal Investigator
 DBT Project
 Tezpur University

Finance Officer
 Tezpur University
 OSD Finance
 Tezpur University

Registrar
 Tezpur University
 Registrar
 Tezpur University

Principal Investigator
 "Multi Functional by bridging applications."
 DBT Project.
 DEPARTMENT OF PHYSICS.

2012 June	0.00	16000.00	0.00
-----------	------	----------	------

Details of expenditure incurred on Manpower

(Details should be given separately for each position)

- Post sanction (provide details of each post in similar following fashion)
- Date of appointment and Date of relieving
- Monthly stipend, HRA etc. Paid.
- Year wise total payments made.

I. Financial year	II. Financial year	III. Financial year	IV. Financial year
2009-10	2010-11	2011-12	2012-13
Rs.135745.00	Rs.240000.00	(-)Rs.144000.00	Rs.519200.00
Grand total Rs.			
			750945.00

Please indicate if there was any deviation as against the DBT sanction and reason there of.

(P. Deb)

Principal Investigator
DBT Project
Tezpur University

Finance Officer
Tezpur University

OSD Finance
Tezpur University

Registrar
Tezpur University

Registrar
Tezpur University

Principal Investigator

"Multi Functional by bridging applications."

DBT Project.

DEPARTMENT OF PHYSICS,
TEZPUR UNIVERSITY

0.00

16000.00

0.00

0.00

0.00

0.00

0.00

0.00